JOURNAL OF MATERIALS SCIENCE 15 (1980) 1153–1166

The structure of glasses in the TeO_2-P_2O_5 system

S. NEOV, I. GERASIMOVA
Institute of Nuclear Research and Nuclear Energy, Bulgarian Academy of Sciences, 1113-Sofia, Bulgaria

V. KOZHUKHAROV, M. MARINOV
Institute of Chemical Technology, 1156-Sofia, Bulgaria

The co-effects of two glass-formers in the TeO_2–P_2O_5 system are studied on the basis of neutron diffraction data. The curves for the radial distribution function (RDF) obtained show a high extent of destruction of the short-range order in the tellurite matrix, while the basic co-ordination PO_4 polyhedron remains unchanged. The co-ordination number (cn) of the Te atom changes from 4 to 3 + 1 and marked tendency towards elongation of the Te–O distances over 2.3 Å is observed. The considerably higher stability of the PO_4 polyhedra and their strong influence on the TeO_4 polyhedra is established. The observed "smearing" effect of the Te–Te, Te–second O and O–second O distances in the range of 3.8 to 3.9 Å in other tellurite glasses is also characteristic of this system. A structural interpretation of the liquid–liquid immiscibility on the short-range order level in the system is given. A critical composition with 26 ± 5% of the second glass-former is established, above which concentration a stable immiscibility in the tellurite systems is observed. An attempt is made to construct two adequate structural models (microhomogeneous and microheterogeneous) for the short-range order in the glasses studied.

1. Introduction

The basic co-ordination polyhedron of α–TeO_2 (paratellurite) is considered as a trigonal bipyramid with one unoccupied equatorial position [1–3]. The tellurium atom is four-fold co-ordinated in relation to oxygen, the remaining valence electrons forming a free electron pair. The larger space which it requires leads to deformation and a decrease in the Te–O–Te angles, and its stereochemical activity has an essential effect on the structure and properties of tellurite glasses.

The neutron diffraction investigations [4, 5] were intended to clarify some basic aspects of the nature of tellurite glasses. On the basis of the experimentally obtained RDFs, models were constructed which indicate that at the vitreous transition the most sensitive are the Te–Te and Te–second O distances in the region about 3.9 Å. It was established that the basic co-ordination polyhedron is a TeO_4 group which can be found in the glass in three states: trigonal bipyramids, tetrahedra (SR-model) and trigonal bipyramids with three strong bonds and one elongated axial bond. In the last state, as a consequence, a 3 + 1 co-ordination of the Te atom is required. The presence of TeO_3 polyhedra in the glass is also possible, but their contribution to the RDF is negligible and depends strongly on the modifier concentration. According to the SR-model the role of the modifier in the vitreous transition is exceptionally important. In principle, it consists in its incorporation in the active structural regions between two $[-\underset{|}{\overset{|}{\mathrm{Te}}}-{}_{\mathrm{ax}}\mathrm{O}_{\mathrm{eq}}-\underset{|}{\overset{|}{\mathrm{Te}}}-{}_{\mathrm{eq}}\mathrm{O}_{\mathrm{ax}}-\underset{|}{\overset{|}{\mathrm{Te}}}-]_{\infty}$ chains or layers thus causing their deformation and rupture. In the places of rupture, TeO_4 tetrahedra are formed on the side of the stereo-

0022–2461/80/051153–14$03.40/0

chemically active free electron pair of the Te atom. This, in turn, leads to the formation of stable $-\overset{|}{\underset{|}{\mathrm{Te}}}-\mathrm{O}-\mathrm{M}$ ion-covalent bonds, which are realized through bridging oxygen ions. A strong influence of the modifier on the Te–O–Te angle between two polyhedra was established. These structural features were proved only for glasses which contain modifying oxides [4, 5].

The present investigation attempts to study by neutron diffraction methods a tellurite system which contains a second glass-former. Such systems exhibit a stable phase separation [6–8] and are of undoubted scientific interest. For this purpose we have chosen the typical immiscible TeO_2–P_2O_5 system.

P_2O_5 is known [9, 10] to occur in three different crystalline forms as well as in the amorphous state [11]. All these forms are built from PO_4 tetrahedra, which share three of their corner oxygen atoms with adjacent tetrahedra. The rhombohedral form of P_4O_{10} crystallizes in the space group $R3_c$;T_d symmetry with lattice constant $a = 7.4$ Å, $\alpha = 87^\circ$ and $Z = 4$. Important interatomic distances are: –P–O– bridge, from 1.60 to 1.64 Å, and abnormally short –P=O bond from 1.40 to 1.42 Å. On heating above 450° C the metastable H-form turns into a stable O′ (rhombic) form. Because of the great stability of the latter, it is used to calculate the $\mathrm{RDF}_{\mathrm{theor}}$ (see Fig. 5 curve 10) for quasicrystalline P_2O_5.

The structure of the phosphate glasses has not been extensively studied by diffraction methods. For example, glass-like Graham's salts have been studied by Brady [12] who obtained cn = 4.2 using X-ray diffraction. The basic unit in the structure is a PO_4 tetrahedron. In $NaPO_4$ glass, each tetrahedron was the origin of a network extending out in two directions, i.e. incipient stage of a layer structure. Milberg and Dally [13] assumed that the metaphosphate chains are also built up of PO_4 tetrahedra. Soclakov *et al.* [14] assumed that each P atom is surrounded by 4 oxygen atoms and each PO_4 polyhedron is connected by two vertices with another two neighbouring tetrahedra.

No results have been reported in the literature on any structural investigation of the TeO_2–P_2O_5 system: only the crystal structure of the ditellurium(IV)-trioxid-hydrogenphosphate has been determined [15]. The orthorhombic $Te_2O_3(HPO_4)$ has the space group $P_{ca}2_1 - C_{2V}^5$ with $a = 10.23$, $b = 7.01$, $c = 7.92$ Å and $Z = 4$. The tellurium atoms show an one-sided coordination to four oxygen atoms which is typical for Te(IV). The average Te–O_{ax} distances are 2.07 and 2.06 Å, and the average Te–O_{eq} distances are 1.89 and 1.85 Å, respectively.

The present paper aims at clarifying the following problems:

(1) determination of the form and extent of deformation of the elementary structure unit;

(2) characterization of the role and mechanism of the mutual influence of two glass-formers as a function of their concentration;

(3) determination of the distances above which no order is observed;

(4) structural interpretation of the phase separation and determination of the factors ruling the phase-separation process in its initial stages;

(5) establishment of structural models which, on the one hand, characterize the structural features of chemically homogeneous systems and, on the other, clarify the initial stage of nucleation in tellurite glasses.

2. Theory

The structural information on glasses is mainly contained in the RDF of the atomic density $\rho(R)$. According to Debye the oscillations of $\rho(R)$ about its mean value ρ_0 are given by the equation

$$F(R) = 4\pi R^2(\rho(R) - \rho_0) = \frac{2R}{\pi}\int_0^\infty Qi(Q)\sin QR\,\mathrm{d}Q \qquad (1)$$

where Qi is the so-called normalized intensity equal to $(I(Q) - I_\infty)/(I_\infty - I_0)$, I_∞ and I_0 are the values of the scattered radiation $I(Q)$ at $Q \to \infty$ and $Q = 0$, respectively. The conditions of the diffraction experiment considerably restrict the integration limits. The maximum value of the upper limit cannot exceed $4\pi/\lambda$, and its actual value is determined by $Q_{\max} = 4\pi\sin\theta_{\max}/\lambda$, where θ is the half scattering angle. While the change in the lower limit has a weak effect on $F(R)$, the integration cut-off leads to the appearance of spurious peaks symmetrically positioned about the maxima at distances $\Delta R = \pm 2.5\pi/Q_{\max}$ [16]. For their reduction, modifying functions, $M(Q)$, are introduced. In the numerical integration of Equation 1 we have used the function proposed by Lorch [17]:

$$M(Q) = \sin\frac{\pi Q}{Q_{\max}}\Big/\frac{\pi Q}{Q_{\max}}.$$

The values I_∞ and I_0 are found from the experimental diffraction curve. From the condition

$$\lim_{R\to\infty}\rho(R) = \rho_0$$

it follows that

$$I_\infty \approx \frac{2}{Q^2_{\max}}\int_0^{Q_{\max}} QI(Q)\,\mathrm{d}Q. \tag{2}$$

The value of I_0 is determined by averaging $I(Q)$ at the minimum values of Q, at which the experimental curve becomes almost parallel to the abscissa.

The assumption that the thermal neutron scattering is elastic in non-crystalline substances is an approximation which is better the greater the mass of the scattering nucleus. A partial compensation for the non-elasticity may be achieved using the corrections derived by Placzek [18]:

$$I(Q) = \overline{b^2}\left[1-\frac{2\sin^2\theta}{\mu}\left(1-\frac{1}{\mu}\right)+\frac{\bar{K}\cos 2\theta}{3\mu E_0}\right] + \bar{b}^2\int_0^\infty \rho(R)e^{iQR}\,\mathrm{d}R \tag{3}$$

Here $\mu = M/m$ is the ratio of the masses of the scattering atom and the neutron, E_0 is the initial neutron energy, $\bar{K}$ is the average kinetic energy per scattering atom.

For complicated systems, comparison of the experimentally obtained RDF with the theoretical model curves is the only way to interprete the radial function. In the case of glassy objects, the structural diffusion model proposed by Prins [20] is particularly fit for modelling. In this model it is assumed that translational motion of atoms is absent, but they are randomly shifted from their equilibrium positions in the corresponding crystal lattice. At that, with the increase of the distance R between a given pair of atoms the shift from the equilibrium position will be a sum of random quantities, i.e. it will be proportional to R. If a_i denotes the halfwidth of the distribution centred at R_i which we assume Gaussian, then $a_i^2 \sim 4DR_i$. By analogy with the usual diffusion the coefficient, D is called the structural diffusion coefficient. The theoretical RDF ($\mathrm{RDF_{theor}}$) is a sum of all possible interatomic distributions. For a binary system it has the form:

$$4\pi R^2\rho(R) = 4\pi R^2[n_1\bar{b}_1^2\rho_{11}(R)+n_2\bar{b}_2^2\rho_{22}(R) + 2n_1\bar{b}_1\bar{b}_2\rho_{12}(R)] \tag{4}$$

where $\bar{b}_i$ are the averaged coherent scattering amplitudes for the given compound, n_i are the concentrations of i-type atoms, $\rho_{ij}(R)$ is the distribution of the atoms of type j around i-type atoms. The partial RDFs are sums of Gaussian peaks:

$$\rho_{ij}(R) = \sum_i\sum_j \frac{Z_{i(j)}}{2\sqrt{\pi}a_{ij}}\left(\frac{R}{R_{ij}}\right)^2 e - \left(\frac{R-R_{ij}}{2a_{ij}}\right)^2 \tag{5}$$

where the halfwidths a_{ij} obey the structural diffusion law and $Z_{i(j)}$ are the cns.

3. Experimental details

3.1. Materials and glass preparation

The phase diagrams of the TeO_2–P_2O_5 system is presented in Fig. 1. The immiscibility confines the tendency to transparent glass-formation up to 25.8% P_2O_5. Phase analysis indicates the formation of three new phases: incongruent melting $Te_4P_2O_{13}$, $Te_2P_2O_9$ and a supposed metacompound. REM and SEM investigations established a stable and metastable immiscible dome [8].

The materials used (TeO_2 and P_2O_5) were of Analar grade. X-ray powder diffraction patterns for TeO_2 correlate with paratellurite. In the present study the glasses obtained by the technology described in [8] are shown in Table I. After synthesis, the glass sample was not subjected

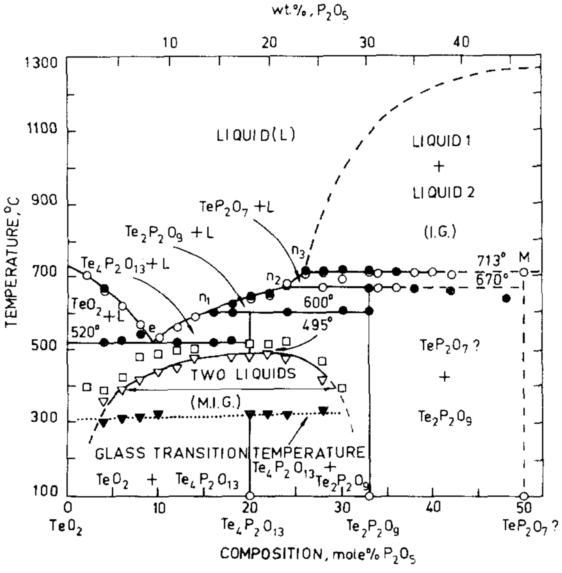

Figure 1 Phase diagram of the TeO_2–P_2O_5 [8].

TABLE I Characteristics of the glass samples

No.	Index	Composition (mol %)		Visual and REM characteristics	Density (g cm^{-3})	Notes
		TeO_2	P_2O_5			
1	TP-1	92.0	8.0	Transparent glass	5.428	Near to eutecticum point
2	TP-2	84.0	16.0	Transparent glass	4.549	Correlate to n_1 peritectic point
3	TP-3	80.0	20.0	Transparent glass with light yellow colour	4.227	Correlate to $Te_4P_2O_9$ compound
4	TP-4	74.0	26.0	Poorly transparent microheterogeneous glass	3.987	Low hygroscopic capacity

to annealing or other additional heat treatment. The densities of the specimens were determined by weighing in air ($t = 16°$ C) and water ($t = 14°$ C).

3.2. Techniques

The presence of a heavy atom in the composition of the vitreous specimens studied favours the use of neutron diffraction methods for obtaining more detailed structural information. The coherent scattering amplitudes for thermal neutrons are very close to each other in the case of Te, O and P: 0.543×10^{-12}, 0.575×10^{-12} and 0.510×10^{-12} cm, respectively, and as a consequence, all kinds of interatomic distances Te–O, Te–Te, P–P, P–O and Te–P will be equally well represented in the RDF. The measurements were performed according to the method described by Neov and co-workers [4, 5]. In spite of the small cross-sections for thermal neutron absorption of the Te, O and P nuclei, an absorption correction was carried out according to the concise formula in [19]. The linear absorption coefficient, μR, was determined experimentally.

3.3. Results

The diffraction spectra measured are shown in Fig. 2. Four diffuse peaks are seen on all the curves; the first peak being a double one. Increase in P_2O_5 concentration produces two main effects. The peak positioned at $Q = 4.5$ Å^{-1} for sample TP-1 gradually shifts towards greater Q-values, and for sample TP-4 is found at $Q = 5.5$ Å^{-1}. The last maximum broadens and almost disappears with increase in P_2O_5 content.

After Fourier transformation, we obtain the function $F(R)$ given in Fig. 3. The $F(R)$ curves calculated up to 12 Å have 11 peaks each, whose distances are given in Table II. Fig. 3a and b and Table II show that the distances which vary most are those of peaks P5, P3 and P7. $F(R)$ curves possess three types of peaks: clearly expressed, with reduced intensity, and masked ones. From

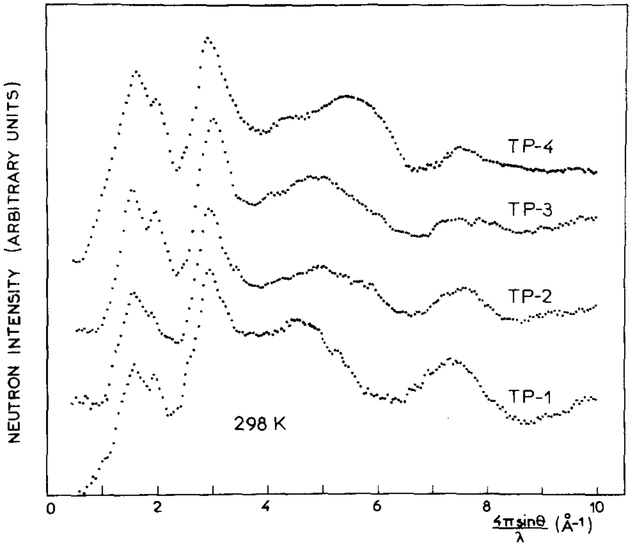

Figure 2 Neutron diffraction spectra of the glasses.

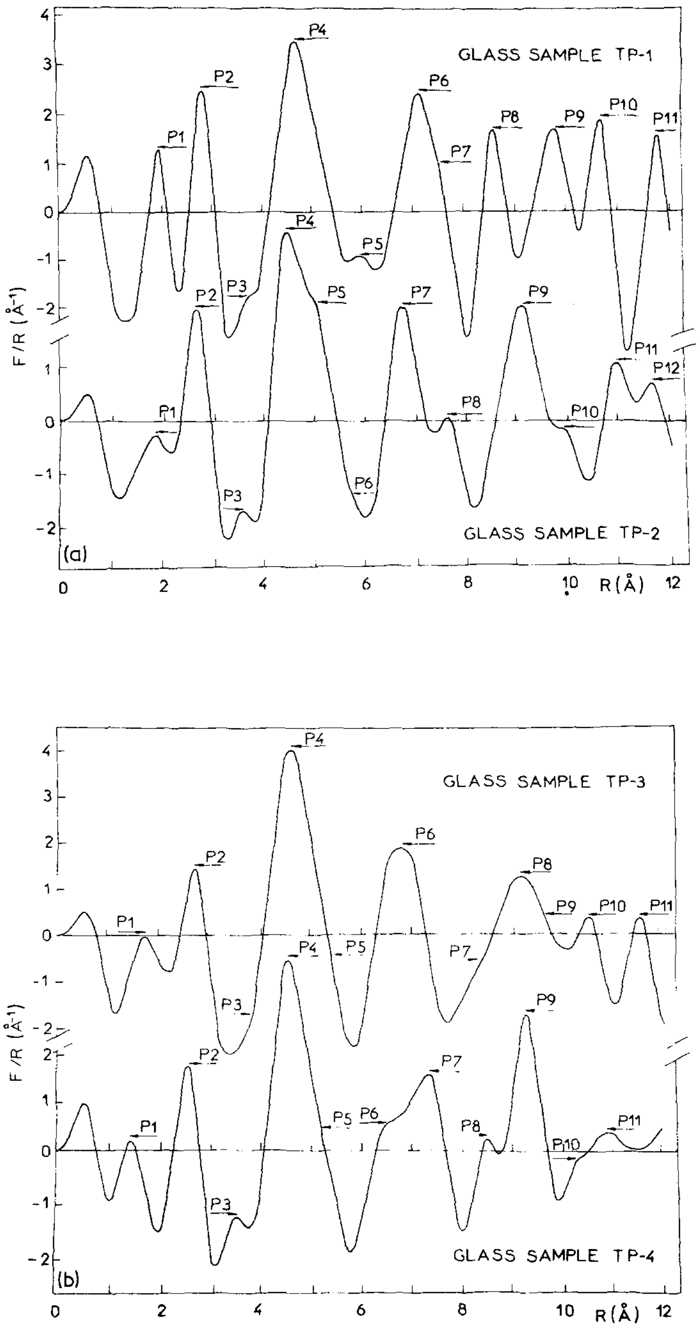

Figure 3 Fourier transform of the diffraction spectra of tellurium glasses: (a) samples TP-1, TP-2, and (b) samples TP-3, TP-4.

TABLE II Interatomic distances in Fourier transform curves

Glass sample	Peaks (Å) for index:										
	P1	P2	P3	P4	P5	P6	P7	P8	P9	P10	P11
TP-1	1.95	2.85	3.84	4.75	6.00	7.15	7.54	8.60	9.30	10.65	11.70
TP-2	1.85	2.65	3.50	4.47	5.05	6.73	7.57	9.05	9.86	10.97	11.65
TP-3	1.65	2.65	3.70	4.55	5.34	6.73	8.33	9.14	9.60	10.48	11.50
TP-4	1.48	2.53	3.53	4.56	5.20	6.55	7.35	8.50	9.25	10.35	10.95

Accuracy of dimensions from P1 to P4 ± 0.06 Å from P5 to P11 ± 0.09 Å

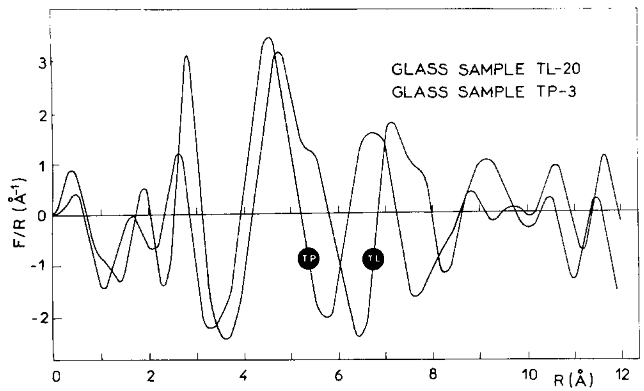

Figure 4 A comparison between Fourier transformation curves of the TL-20 and TP-3 glass samples containing Li_2O 20% and P_2O_5 20%, respectively.

Table II is seen that up to P6 a shift of the peaks is registered towards the lower values of R. This shift is illustrated in Fig. 4. On all the $F(R)$ curves the P4 peak is of highest intensity and has a comparatively wide slope. Because of this the contribution from the neighbouring two peaks is partially masked. Discussion in this region is hampered by the fact that the P4 sums up a considerable number of distances, some of which are very dynamic.

4. Discussion

4.1. General information

A series of theoretically calculated and experimentally obtained RDFs is shown in Fig. 5. All interatomic distances registered up to 7 Å on the RDF are summarized in Table III. Based on the correlation of the curves in Fig. 5, the following points are established:

(a) with increase in P_2O_5 a decrease in the intensity and a shift of peaks P1 and P2 to lower values of R is observed. Of the two peaks, P1 is of markedly higher variability, therefore on curves 5 and 7 a marked widening is observed and the maximum and minimum disappear;

(b) peak P2 is considerably more stable than P1 and P3, but with the increase in concentration of the second component, it is shifted towards low $\bar{R}$ values;

(c) the theoretically well-defined P3 peak is absent from the RDF_{exp} curves.

Since peak P1 results from the radial distribution of the Te–O and P–O distances, we could determine the type and extent of deformation of the elementary structural unit in the glasses. From Figs. 5a and b and 6a for the TeO_2-rich region, it was established that the experimental P1 peak practically remained unchanged. This fact shows that the basic co-ordination scheme, with four-fold co-ordinated Te atom characteristic of α-TeO_2, is preserved in the glass. The TeO_4-group has a marked tendency towards deformation and lability of one of the axial bonds. This lability is sharply increased in the liquid state, where due to kinetic factors the axial bonds easily undergo a dynamic elongation over 2.2 Å. The extent of

TABLE III Interatomic distances in the glasses

Glass sample	Interatomic distances (Å)					cn
	$\bar{R}_{\text{Te—O}}$	$\bar{R}_{\text{O—O}}$	$\bar{R}_{\text{Te—Te;Te—O}}$	$\bar{R}_{\text{O—O}}$	$\bar{R}_{\text{O—O;Te—O}}$	
TeO_2 (theor)	2.0	2.85	3.85	4.80	6.45	4
TP-1 (exp)	1.95	2.85	3.9 (d)*	4.90		4
TP-1 (theor)	2.00	2.90	3.9	4.85	6.50	
TP-2 (exp)	1.90	2.70	3.7 (d)	4.5 (d)	5.25 (d)	
TP-2 (theor)	2.00	2.90	3.9	4.87		
TP-3 (exp)	1.80	2.75	3.9 (d)	4.75	5.5 (d)	
TP-3 (theor)	2.0	2.9	3.85	4.86		
TP-4 (exp)	1.57	2.60	3.7 (d)	4.70	5.5 (d)	
TP-4 (theor)	2.00	2.85	3.85	4.90		
Pure P_2O_5 (theor)	1.6	2.6	3.3?; 3.9	5.0		
Peaks	P1	P2	P3	P4	P5	

*(d) = diffuse.

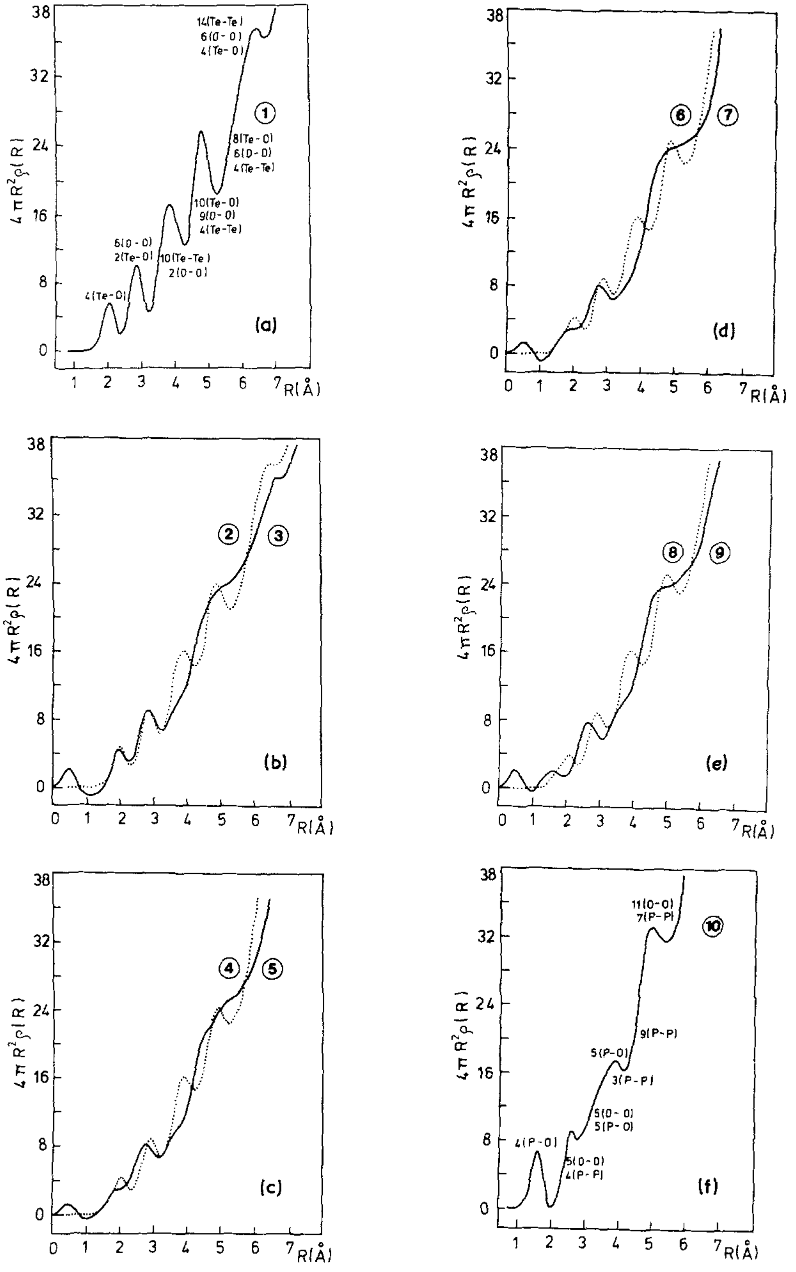

Figure 5 RDF of atomic density of the glasses. Curve 1 (a) present RDF_{theor} of α-TeO_2, curves 3, 5, 7 and 9 are experimentally obtained RDFs of TP-1 (b), TP-2 (c), TP-3 (d) and TP-4 (e) glass samples, respectively, and curves 2, 4, 6 and 8 are related RDF_{theor} (marked by dotted line). Curve 10 (f) is the present RDF_{theor} of P_2O_5.

bond deformation, besides the kinetic factors, is also influenced by the composition, temperature and viscosity of the melt, by the nature of the modifier, as well as by some thermodynamic factors. An undisputable argument in support of this assertion is the fact that in tellurite glasses there are not experimentally recorded marked minima on the RDF between the P1 and P2 peaks at 2.4 Å. This mobility of the distances in the TeO_4 building unit is observed even on theoretical curve 1 in Fig. 5a.

From the above discussion it follows that the elementary structural unit of glasses in the TeO_2-rich region is the trigonal bipyramid with Te–O distances as in paratellurite. The difference consists in that a part of the axial bonds (about 10%) is very dynamic and in the case of a one-sided co-ordination pseudosphere, characteristic of the

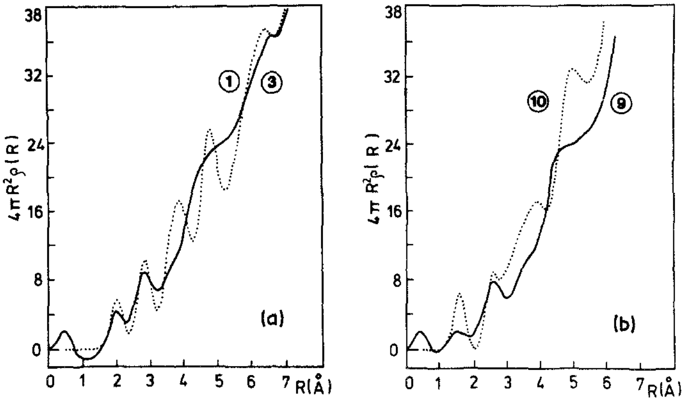

Figure 6 A comparison with theoretical (1, 10) and experimental (3, 9) RDFs of the atomic density (a) RDF of α-TeO_2 and TP-1 glass sample, and (b) RDF of P_2O_5 and TP-4 glass samples.

Te atom, their elongation is realized exceptionally easily, i.e. a 3 + 1 bonding is effected [2, 21]. On the other hand, the structural recombination, which takes place in the active region of the free electron pair of a part of the Te atoms, leads to a strong additional "quasi-equatorial" bonding through a bridging oxygen and to the formation of TeO_4 tetrahedra.

For samples TP-2 and TP-3 a considerable "smearing" of peak P1 on the RDF was observed (see Fig. 5, curves 4 and 6). The reduction of the maximum and minimum is due to the comparatively stronger influence of PO_4 tetrahedra on P1, as well as to the already considerable deformation of the TeO_4 units. The latter undergo a considerable change, at which about 40% of the Te–O distances are elongated up to ~2.35 Å. The co-ordination of the Te atom in this case is preferably 3 + 1. The contribution of the Te–O distance is expressed predominantly in the raising of the minimum at $\bar{R} \approx 2.4$ Å. This phenomenon probably depends on the following factors:

(1) realization of a secondary bonding and increase in the covalence of the bond in TeO_4 polyhedra;

(2) weak interaction between the one-sided co-ordinated Te atoms on the one hand, and through a bridge of PO_4, tetrahedra with other TeO_4 polyhedra from neighbouring chains and layers, on the other;

(3) O_{ax} in the bonds of the type

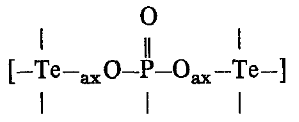

$$[-\underset{|}{\overset{|}{Te}}-{}_{ax}O-\underset{|}{\overset{\overset{O}{\|}}{P}}-O_{ax}-\underset{|}{\overset{|}{Te}}-]$$

is dynamic and, notwithstanding the equal electronegativity of the two cations, it has a definite preference for PO_4 polyhedra and a tendency to secondary bonding with elongation of the 4(Te–O) bond about 2.4 Å.

These characteristic features of a large part of the axial O atom of the TeO_4 polyhedra are illustrated in Fig. 7. Parts of the chains and layers are connected in a three-dimensional random structure by means of a weak axial oxygen bonding, through bridging PO_4 polyhedra. By this means of structure formation, the PO_4 units participate actively not only in the binding between two chains, illustrated in Fig. 8, but also in occupying some of the TeO_4 positions in the tellurite–oxygen chains. Because of the small ionic radius of phosphorus, the P^{5+} ions have a strong electrostatic field and the PO_4-group is characterized by a considerably more compact and stable structure. That is why a small amount of P_2O_5 seems to successfully destroy the stability of Te in Te–O bonds. At the same time, the TeO_4 polyhedron is stereochemically very active on the side of its free electron pair, which contributes to the strong bonding through bridging oxygen. In the presence of a modifier, according to the SR-model, such a bonding is easily realized. In systems with two glass-formers present simultaneously, antagonistic tendencies appear with respect to the formation of the main structure network. Because of their chemical nature (anhydrides of acids, character and strength of the bond, ion-covalency character of the bond, electronegativity of the cations, etc.) they have a strong tendency to conserve the polyhedra, chains and layers and to form their own network. An essential significance for the character of the processes in this type of system is played by the acidity (respectively "basicity") of the both glass-formers. It seems that this property is of great importance in the

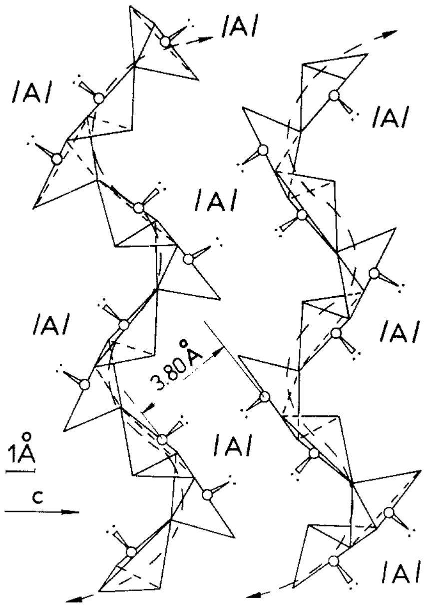

Figure 7 Two tellurium–oxygen chains. $\bar{R}_{Te-Te} = 3.80$ Å. |*A*| represents the active structure region in one direction of the Te atom.

formation of microheterogeneous structure of tellurite glasses in the presence of a second glass-former, and it will be the subject of discussion in the next sections.

The interaction described above between PO_4 and TeO_4 polyhedra changes considerably with in increase in the P_2O_5 concentration. Its higher concentration in the tellurite matrix leads to a drastic break down of the tellurium–oxygen short-range order. From RDF_{exp} it was established that only about 25% of the Te–O distances are preserved unchanged up to 1.9 Å. The fourth Te–O distance is elongated to 2.35 Å on average. In spite of this, the O–O distances remain fixed at about 2.7 Å. This phenomenon contributes to the "oxygen" P2 peak, which is the most stable and is preserved in all the RDF_{exp} curves in Fig. 5. This is due to the fact that

(1) the 2.85 Å maximum is due to O–O distances between the neighbouring TeO_4 polyhedra (see curve 1);

(2) the O–O distances of PO_4 tetrahedra contribute at 2.6 Å (see curve 10);

(3) for different structural arrangements of TeO_4 and PO_4 polyhedra we have variable O–O distances between two polyhedra, but it will be unobservable since the oxygen network packs around $\bar{R} = 2.7$ Å which is near the sum of the oxygen radii.

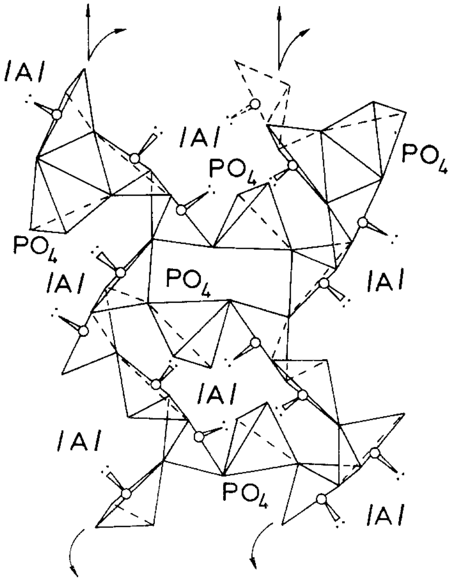

Figure 8 Introduction of PO_4 tetrahedra into tellurium–oxygen chains.

These three cases are presented in Fig. 9. The RDF_{exp} for sample TP-1 indicates predominant $[-\overset{|}{\underset{|}{\mathrm{Te}}}-\mathrm{O}-\overset{|}{\underset{|}{\mathrm{Te}}}-\mathrm{O}-\overset{|}{\underset{|}{\mathrm{Te}}}-\mathrm{O}-\overset{|}{\underset{|}{\mathrm{Te}}}-]$ bonding (Fig. 9a). According to RDF_{exp}, curves 5 and 7, with increase in P_2O_5 concentration, $[-\overset{|}{\underset{|}{\mathrm{Te}}}-\mathrm{O}-\overset{\|}{\underset{|}{\mathrm{P}}}-\mathrm{O}-\overset{|}{\underset{|}{\mathrm{Te}}}-]$ bonding is realized, which is illustrated in Fig. 9b, while the contribution to peak P2 in RDF_{exp}, curve 9, is mainly due to $[-\overset{|}{\underset{|}{\mathrm{Te}}}-\mathrm{O}-\overset{\|}{\underset{|}{\mathrm{P}}}-\mathrm{O}-\overset{|}{\underset{\|}{\mathrm{P}}}-]$ bonding (Fig. 9c). The change in the area of peaks P1 and P2 in RDF_{exp}, curves 5, 7 and 9, should be proportional to the amount of the original components TeO_2 and P_2O_5 (i.e. TeO_4 and PO_4 polyhedra). The observed intensity, unambiguously demonstrates that PO_4 tetrahedra influence the glass structure formation considerably stronger than TeO_4 units. In this aspect, while the deformation of PO_4 is insignificant, the TeO_4 units suffer a strong deformation and in three-quarters of the cases lose their short-range order. The last fact is important for the interpretation of the structural re-grouping in the initial stages of stratification in tellurite systems containing a second glass-former.

Another problem to be solved is the clarification of the structural cause of the vitreous transition

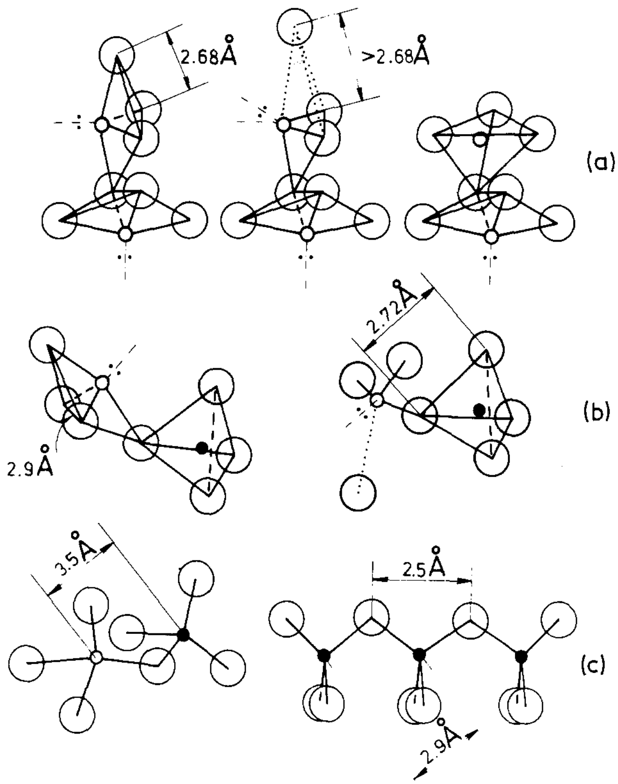

Figure 9 An illustration of the co-ordination state and interaction between TeO_4–TeO_4 (a), TeO_4–PO_4 (b) and PO_4–PO_4 (c) polyhedra; ○ -Te atoms and ● -P atoms.

in tellurite melts and the extent to which the short-range order is preserved in the glass. This problem was discussed in detail by Neov and co-workers [4, 5] but here further consideration is necessary in order to answer the following questions:

(1) Is our criterion [4, 5] for variability of the Te–Te, O–second O and Te–second O distances between two tellurite polyhedra at 3.9 Å valid also for glass-like systems without modifiers?

(2) If the phenomenon is present in the system studied what is the extent of diffuseness of the distances?

(3) How is this important criterion for glass-formation of tellurite systems influenced by the concentration of the second component?

The answer to these questions can be obtained by analysing peaks P2 to P5. From Table III and Figs. 5 and 6 it is seen that the distances about 3.9 Å are very diffuse and vaguely expressed. The Te–Te, Te–P, O–second O and Te–second O bonds have just that distance. From Fig. 5, curve 10 it follows that here we should also have a contribution from the P–P distances between two neighbouring polyhedra. This is partly realized in RDF_{exp} curve 9, where there is a more marked maximum at 3.7 Å rather than weak fluctuations in this region as in the RDF_{exp} curves 3, 5 and 7. The diffuseness of these distances shows that this is one of the main causes of vitreous transition. For example, the Te–Te distances along the *c*-axis in paratellurite are most sensitive to the addition of a second component. This is due to the fact that here microcavities exist, which are able to accept the polyhedra of the second component. The interaction of these polyhedra in the structurally active regions between the chains favours the structural recombination as well as the deformation of a part of the Te–O bonds. The differences between the RDF_{theor} and RDF_{exp} illustrated in Fig. 5 show that with the increase in P_2O_5 concentration the distances which contribute in peak P2 change towards lower values of R, unlike the distances around 5 Å, which are not affected significantly by the concentration of the second component.

As a conclusion we can note that the established criterion for variability of the distances between two neighbouring units is observed in the system under consideration for all distances but to a different extent. Most sensitive to changes seem to be the Te–Te, Te–P and O–second O distances. The shape of the RDF_{exp} curves for the tellurite glasses studied so far shows that this criterion is valid irrespective of the chemical nature and behaviour of the second component. The established diffuseness of the distances is a characteristic feature of the tellurite bonds in the glasses. This feature also influences the conservation of the short-range order which does not exceed 10 Å in the glasses.

4.2. Structural interpretation of the immiscibility

An essential influence on the immiscibility in glasses is exerted by the structural interaction between the components. Warren and Pincus [22] were the first to apply the ideas of crystal chemistry to the study of phase separation processes in vitreous systems. They have established that given a modifier and a glass-former, the two compete predominantly with respect to the unsaturated oxygen ions.

An important factor for the development of the liquation process in glasses is the electrostatic bond strength (EBS) defined as Z/cn where Z is the charge of the cation. It is known that phase separation is typical for bond strength equal to $\frac{3}{8}$, $\frac{1}{2}$. This shows that a modifier should have a variable bond strength with oxygen, in order to cause immiscibility. In liquation systems with a modifier, the stronger the modifier–oxygen bond, the stronger is the tendency to phase separation. A necessary condition is that the EBS be smaller than $\frac{1}{2}$ and greater than $\frac{5}{6}$. Irrespective of these demands, however, the oxygen co-ordination polyhedron of the cation must be incompatible with the cation of the network-former.

Another important factor in the liquation process is the ionic field strength (IFS). Both cations in the studied system tend to keep their co-ordination polyhedra, chains and layers stable. There will be no liquation if the cation–oxygen field strength is too large or, on the other hand, negligible. Thus it is important to have, as a measure of the liquation process, a quantitative evaluation of the bonding of the Te and P ions with oxygen. Such a quantitative measure is the difference in the field strength. According to Levin [23] there will be no phase separation if IFS is greater than 0.85 or smaller than 0.06 to 0.02. After Scholze [24], for the two cations in the system studied, we have $\mathrm{IFS} = 0.071$, which satisfies the condition for a liquation process to proceed [23].

The structural characteristics of the two polyhedra were discussed above. Apart from the high electrostatic charge of the P^{5+} ions, the double –P=O bond favours the closest packing of the polyhedron and consequently sharply increases the necessary minimum energy for breaking off the bonds. This is one of the causes for the liquation in a binary phosphorous system to be absent or extremely rare. Consequently, it is logical to seek the causes in the structural features of the TeO_4 polyhedra and their interactions with the second glass-former. Essentially, the main structural changes which TeO_4 polyhedra undergo in the initial stages of the liquation process are the following.

(1) The TeO_4 unit is a one-sided co-ordinated polyhedron, with a free electron pair and highly mobile axial bonds.

(2) Such a co-ordination pseudosphere of the Te atom favours secondary bonding, i.e. an easy variability of the bond strength with respect to oxygen exists. The latter point follows from the high deformation of the Te–Te, Te–second O and O–second O distances.

(3) The active interaction of TeO_4 polyhedra on the side of their free electron pair with the unsaturated oxygen ions, cannot lead to the formation of a strong –Te–O–P– ion-covalent bonding, as in the presence of a modifier [5].

(4) With two glass-formers present simultaneously, because of the antagonistic tendencies for preservation of their own networks, a space structural differentiation of the polyhedra takes place in the initial stages of the phase separation.

(5) The weaker acidity of TeO_2 (anhydride of the weak H_2TeO_3 acid) compared to P_2O_5 also favours easier attacking of the chains in α-TeO_2. In this aspect TeO_2 probably plays the role of a modifier, i.e. it appears more "alkaline" than the second glass-former.

Owing to the above causes the different glass-forming polyhedra have no inclination to associate amongst themselves. This gives one grounds to consider that a space-structural differentiation of the polyhedra, groups, chains and layers takes place, i.e. a liquation process occurs.

It should be noted, however, that there is a possibility of the formation of low-polymerization phosphate groups at low P_2O_5 concentration. Their formation is influenced by two factors: first, decrease in the extent of polymerization of the phosphate structural patterns, because of the essential incorporation of the second component in the tellurite network, and second, the apparent incompatibility of the structural units of the two glass-formers. At higher P_2O_5 concentrations, the polymerizing phosphate forms groups and chains easily from microscopic drop-like aggregates, locked by the defective tellurite matrix which has a considerably higher stereochemical instability.

4.3. Description of the models

Depending on the change in the P_2O_5 amount and the behaviour of the glasses, two structural models may be proposed on the basis of the RDFs obtained. The first presupposes microhomogeneity and is valid for glasses in the TeO_2-rich region. The second model describes the mechanism of the initial stage of microheterogeneity in glasses of the $TeO_2-G_nO_m$ systems (where G_nO_m is a glass-former) and is valid in the G_nO_m-richer regions.

For microhomogeneous glasses, the structural model illustrated in Fig. 10 should be considered reliable. Besides stereochemically, the model can be represented by symbols, e.g. Fig. 11. This means of representation, however, does not enable the structural angular deformation and the stereo-ordering in tellurite glasses to be displayed. Because of this, in the present work and in the future we shall use the stereochemical representation predominantly.

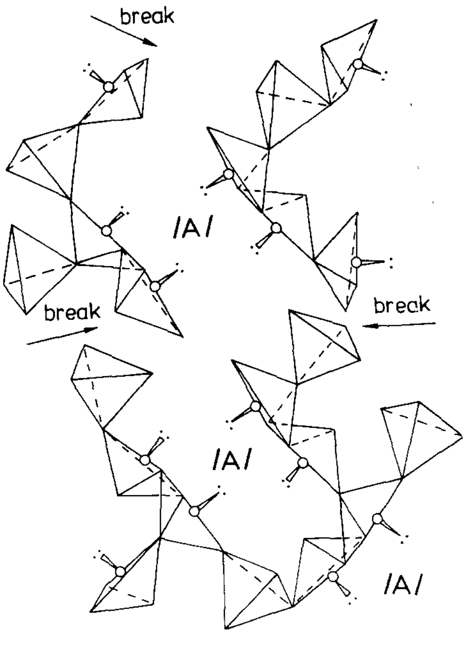

Figure 10 A model illustrating the nature of the atomic arrangement in the TeO_2-rich clear glass region.

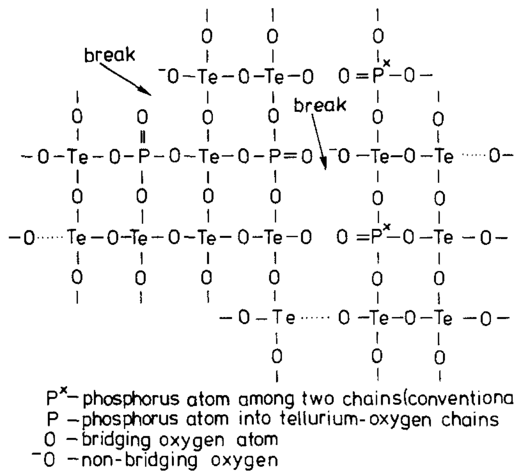

Figure 11 Representation of the model by symbols.

The model may be described as follows: glass-formation in tellurite systems takes place when the structure is highly defective. It is realized mainly through deformation of the bonds, angles and, in places, breaking of the $[-\overset{|}{\underset{|}{\mathrm{Te}}}-\mathrm{O}-\overset{|}{\underset{|}{\mathrm{Te}}}-\mathrm{O}-\overset{|}{\underset{|}{\mathrm{Te}}}-]_\infty$ chains and the corresponding layers. Apart from the case of the SR-model, bonding rupture is also realized when incorporation of PO_4 polyhedra in the tellurite chains takes place, according to the mechanism illustrated in Figs. 10 and 11. Independent of this, the greater part of the PO_4 groups is implanted predominantly in the active tetrahedric holes between TeO_4 chains. By this method of bonding the covalency of the wave-like chains and layers increases. The layers interact weakly among themselves through –P–O–Te– bridging oxygen bonds. The PO_4 tetrahedra positioned between the layers do not contribute to the strengthening and formation of a stable ion-covalent structure, because of the tendency to co-ordination saturation in themselves. In addition to the connection of the type $[-\overset{|}{\underset{|}{\mathrm{Te}}}-\mathrm{O}-\overset{\|}{\underset{|}{\mathrm{P}}}-\mathrm{O}-\overset{|}{\underset{|}{\mathrm{Te}}}-]$ in Figs. 10 and 11, it is shown that a certain number of PO_4 tetrahedra can occupy site positions by incorporation in the tellurite chains and layers. In this way the mobility of the polyhedra and chains sharply increases. With increase in the concentration of the second glass-former, a greater and greater part of the PO_4 units is distributed between the wave-like layers. Thus two types of bonding of the phosphorus ions is realized: P atoms in tellurite chains and P atoms incorporated between chains and layers.

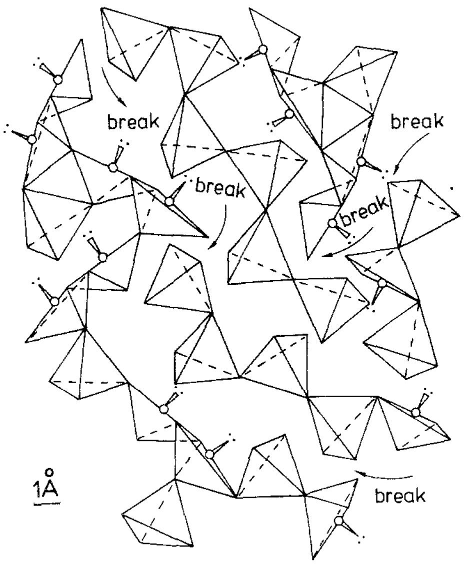

Figure 12 SI-model illustrating the nature of the initial steps of immiscibility in the P_2O_5-rich glass region.

The first contribute to the breaking of the chains and high deformation of the structure. This takes place as early as the introduction of 2% P_2O_5 at which the tellurite melt is easily overcooled. This shows that at low concentrations, the PO_4 polyhedra essentially contribute to the co-ordinational asymmetry of the tellurite structural patterns.

The second type of phosphorus atoms (denoted by P^x) distribute themselves between tellurite chains and layers having a marked tendency to preserve their own co-ordinational bonding. It could be concluded that both methods of bonding stimulate the creation of non-bridging oxygen ions of the type –Te–O, while the non-bridging oxygen ions to which the PO_4 group contributes, are predominantly of the –P=O type.

On the basis of the detailed neutron diffraction and ESR [25] studies carried out in the P_2O_5-rich region, a structural incompatibility model (SI-model) is presented in Fig. 12. The model gives a satisfactory description of the mechanism of the initial microheterogeneity in tellurite glasses. This accounts for the main structural factors which stimulate the occurrence of stable liquation in the initial phases on the short-range order level and could be described as follows.

With the increase in P_2O_5 concentration, a greater and greater number of PO_4 polyhedra attack the tellurite chains and layers, but notwithstanding the large deformation of the structure, it has the tendency to preserve its character and high covalency. The rupture of the tellurite network is realized independent of the preservation of the phosphate chains and layers, at which, because of their high stability, the PO_4 units exert their influence far before the addition of an equivalent amount of the two glass-formers. As far as certain regularity is concerned, in the case of tellurite glasses with a second glass-former, there should be a stable liquation starting with a critical composition within the limits 26 ± 5% G_nO_m. The variation of these limits depends on the conditions of glass-formation (kinetic factors of the vitreous transition), on the type of the phase diagram, the electrostatic bond strength as well as on the structural specificity, acidity, conservation and other characteristics of the polyhedra.

The SI-model can be presented as a high covalent, deformed structure between wavy layers which has very dynamic Te–P, Te–Te, Te–second O, O–second O distances and bridging bonds between them. On its own part, this favours the weak interaction between groups and atoms belonging to different chains and layers. Parallels to the broken tellurite chains, and also perpendicular to them, fragments of chains of the second glass-former are incorporated in addition to polyhedra. The second glass-former causes strong structural disorder because of its tendency to own-network formation. The functions of the two glass-formers are modified, depending upon their concentrations. The PO_4 units act structurally, differentiating even before the equimolecular composition is reached because of their stronger acidity and stability. Owing to their structural specifities, the TeO_4 polyhedra are not in a position to significantly resist the influence of the second glass-former. Thus, in this way, each forms its own microstructure. The strong antagonism in the binding leads to spacial structural differentiation, illustrated in Fig. 12. The SI-model describes the procedure of an initial stage in the structural regrouping of several polyhedra or chain fragments which is the main prerequisite for the development of microheterogeneity. This phenomenon is not observable by electron microscopy at this stage in the structural differentiation.

5. Conclusions

The results obtained may be summarized as follows.

(1) The TeO_2-rich glasses are microhomogeneous and preserve the basic structural unit of the

α-TeO_2. The RDF_{theor} calculated as a sum of the RDFs for TeO_2 and P_2O_5 depending upon their concentrations shows very good agreement with the shortest distances in the experimental curve for $4\pi R^2 \rho(R)$.

(2) In compositions containing $> 15\%$ P_2O_5, a disproportionately fast decrease in the contribution from the TeO_4 bipyramids in the total RDF curve is observed. The proposed structural model shows the best agreement with experiment if it is supposed that 40% of the Te–O distances are elongated to 2.35 Å. Simultaneously, the oxygen network of the glass is built up with average O–O distances of about 2.7 Å.

(3) The Te–Te and Te–second O bonds in the region about 3.9 Å suffer strong deformation, and the theoretical peak is not observed on the RDF_{exp} curve. PO_4 tetrahedra are incorporated between the chains as well as in them, but because of the space-structural differentiation of the polyhedra, a fast distribution of the tellurite network takes place.

(4) At higher P_2O_5 amounts the characteristic peak at 1.95 to 2.0 Å disappears. In its place a maximum appears at $\bar{R} = 1.6$ Å which is characteristic of the average P–O distance. The best approximation to the experiment gives the assumption that 75% TeO_4 units are greatly deformed. The deformation consists in elongation of the R_{Te-O} to 2.35 Å, distortion of the angles and breaking of the –Te–O–Te– chains. The oxygen network maintains its stability with O–O distances of approximately 2.6 to 2.7 Å.

References

1. J. LECIEJEWICZ, *Z. Kristall.* **116** (1961) 345.
2. J. ZEMANN, *ibid* **127** (1968) 319.
3. O. LINDQVIST, *Acta Chem. Scand.* **22** (1968) 977.
4. S. NEOV, I. GERASIMOVA, K. KREZHOV, B. SYDZHIMOV and V. KOZHUKHAROV, *Phys. Stat. Sol. (a)* **47** (1978) 743.
5. S. NEOV, V. KOZHUKHAROV, I. GERASIMOVA, K. KREZHOV and B. SYDZHIMOV, *J. Phys. (C) Solid State* **12** (1979) 2475.
6. W. VOGEL, H. BURGER, G. WINTERSTEIN, CH. LUDWIG and W. JACKEL, *Silikattechnik* **25** (1974) 209.
7. V. KOZHUKHAROV, M. MARINOV and V. V. ON, Proceedings VIII National Conference of TNTM, Sofia (1975).
8. V. KOZHUKHAROV, M. MARINOV and J. PAVLOVA, *J. Mater. Sci.* **13** (1978) 997.
9. E. THILO, in "Advances in Inorganic Chemistry and Radiochemistry", Vol. 4, edited by A. Sharpe Emelénsa, (Academic Press, New York, 1962) p. 57.
10. H. RAWSON, "Inorganic Glass-Forming System" (Mir, Moscow, 1970) p. 161.
11. W. HILL, G. FAUST and S. HENDRICKS, *J. Amer. Chem. Soc.* **65** (1943) 794.
12. W. BRADY, *J. Chem. Phys.* **28** (1958) 48.
13. M. MILBERG and M. DALLY, *ibid* **39** (1963) 2966.
14. A. SOKLAKOV, N. PORTNOVA and V. NECHAEVA, SB. "Stekloobrasnoe sostoanie" (1969) (Nauka, Leningrad, 1971) p. 144.
15. H. MAYER, *Z. Kristall.* **141** (1975) 354.
16. R. HOSEMAN, *Z. Phys. Chem.* **41** (1964) 3/4.
17. E. LORCH, *J. Phys. (C)* 9 (1969) 229.
18. G. PLACZEK, *Phys. Rev.* **86** (1952) 377.
19. K. RONSE, M. COOPER, E. YORK and A. CHAKORA, *Acta Cryst.* **A26** (1970) 682.
20. G. PRINS, *Naturwiss.* **19** (1931) 435.
21. M. TRÖMEL' private communication.
22. B. WARREN and A. PINCUS, *J. Amer. Ceram. Soc.* 23 (1940) 301.
23. E. LEVIN, *J. Amer. Ceram. Soc.* **50** (1967) 29.
24. H. SCHOLZE, "Glass: Natur, Structure und Eigenschaften" (Springer-Verlag, Berlin, Heidelberg, New York, 1977) S.91.
25. B. CAMARA, V. KOZHUKHAROV and H. OEL, *Glastechn.* **53** (1980) to be published.

Received 14 August and accepted 24 September 1979.